2012

Non-Gaussian Anisotropic Diffusion Processing for Medical Imagining Using the OsiriX DICOM Viewer

Jonathan Blackledge
Technological University Dublin, jonathan.blackledge@tudublin.ie

Matthew Blackledge
Institute of Cancer Research and Royal Marsden Hospital

Jane Courtney
Technological University Dublin, jane.courtney@tudublin.ie

Recommended Citation

Blackledge, J., Blackledge, M., Courtney, J.:Non-Gaussian Anisotropic Diusion Processing for Medical Imagining Using the OsiriX DICOM Viewer. *International Society for Advanced Science and Technology (ISAST) - Transaction on Computing and Intelligent Systems*, vol: 4, issue: 1, pages: 24 - 31, 2012. doi:10.21427/D74G9P

Non-Gaussian Anisotropic Diffusion for Medical Image Processing using the OsiriX DICOM

J. M. Blackledge, M. D. Blackledge and J. N. Courtney

***Abstract*— We present a method for reducing noise in CT (Computed Tomography) and MR (Magnetic Resonance) images that, in addition to other noise sources, is characteristic of the numerical procedures required to construct the images, namely, the (inverse) Radon Transform. In both cases, MR imaging in particular, an additional noise source is due to non-stationary diffusion thereby predicating use of the Anisotropic Diffusion Method for noise suppression. This method is based on a diffusion model for noise generation where the Diffusivity is taken to be non-isotropic (inhomogeneous) or anisotropic and is, in the absence of *a priori* information, computed through application of an edge detection algorithm. We extend this approach to include the effect of fractional diffusion (when the underlying statistical model associated with the diffusion process is non-Gaussian) and derive a corresponding Finite Impulse Response filter. The algorithms developed are implemented using the OsiriX DICOM (Digital Imaging and Communications in Medicine) viewer, a high performance open source image data visualization system for the development of processing and visualization tools. An OsiriX Plugin *Image Filter* is provided for interested readers and practitioners to apply.**

***Index Terms*— Medical imaging, Digital Imaging and Communications in Medicine, Computed Tomography, Magnetic Resonance Imaging, Non-Gaussian Anisotropic Diffusion, Noise suppression, OsiriX DICOM viewer.**

I. Introduction

The aim of a noise reduction algorithm is to enhance the fidelity of an image by eliminating features that are random and uncorrelated while retaining resolution on those features that are noise free. The reason for this may be to enhance the visual clarity of an image for visual inspection and/or digital image analysis for object segmentation and feature selection. As a general rule of thumb, noise tends to corrupt the higher frequency content of an image where the energy of the data spectrum is usually lower. Thus, a way of reducing noise is by attenuating the high frequency components of the data over a range of frequencies which can be selected and adjusted to provide an optimum result, subject to some predefined image quality criterion. This can be achieved by applying a lowpass filter. A well known and commonly used lowpass filter is the Gaussian function which yields a 'Gaussian Blur' and, on a physical basis, is related to classical diffusion processes. This is because the Point Spread Function of an image generated by the diffusion of light is a Gaussian function, a result that can be derived by considering the propagation and interaction of light to be based on a random walk process. The underlying equation for the intensity of light is then given by the diffusion equation.

An important assumption associated with the application of a Gaussian blur filter is that the noise content of the image is additive and homogenous. This is to say that the statistical distribution of the noise is homogeneous throughout the image plane and does not change over the spatial extent of the image in terms of scale, width and/or distribution type. Even if this is the case, and, the noise associated with the generation of an image can be quantified (in a statistical sense), application of a Gaussian lowpass filter reduces at the expense of resolution on correlated features, patterns and textures.

In this paper, we review the Anisotropic Diffusion Method for noise reduction illustrating the relationship between this method and the Characteristic Function that is used to define an anisotropic Gaussian random walk process. This process is then extended to include the 'non-Gaussian' case based on Lévy's (symmetric) Characteristic Function which introduces the 'Lévy index'. By re-working the Anisotropic Diffusion Method for this case, we derive a new (Lévy index dependent) Finite Impulse Response (FIR) filter which is our original contribution to the field. The algorithms developed are applied to CT (Computed Tomography) and MR (Magnetic Resonance) and implemented in the OsiriX DICOM (Digital Imaging and Communications in Medicine) Viewer to produce a new image filter (an OsiriX Plugin) and an original application in the area of medical imaging.

Since the focus of this work is on noise reduction, a brief discussion of the sources of noise in CT and MR images is given as detailed in [1], for example. We start by providing a brief overview of DICOM which is given in the following section. However, it should be noted that diffusion based models have a range of applications that transcend image noise reduction especially in MR imaging where the process of diffusion is used to generate a form of image analysis known as Diffusion Weighted and Tensor Diffusion (MR) imaging, e.g. [2], [3], [4] and [5]. The approach considered in this paper may have additional applications in this area of imaging, details of which will be published elsewhere.

II. Digital Imaging and Communications in Medicine

The Digital Imaging and Communications in Medicine (DICOM) standard is used for the exchange of medical images and related information. DICOM is a standard with several

Manuscript completed in October, 2012.

Jonathan Blackledge (jonathan.blackledge@dit.ie) is the Science Foundation Ireland Stokes Professor at Dublin Institute of Technology. Matthew Blackledge (mattyblackledge@gmail.com) is a Research Fellow at the Cancer Imaging Centre, Institute of Cancer Research and Royal Marsden Hospital, UK. Jane Courtney is a Lecturer in the School of Electrical Engineering Systems, Dublin Institute of Technology, Ireland.

levels of support including an image exchange underlying information model and information management services[1] [6].

DICOM was introduced in 1993 after some ten years standards development from the early 1980s when only manufacturers of CT or MR imaging devices could decode the images that the early machines generated. DICOM differs from some, but not all, data formats in that it groups information into data sets. Thus, a file of a chest X-Ray image, for example, actually contains the patient ID within the file, so that the image can never be separated from this information by mistake. This is similar to the way that image formats such as JPEG can also have embedded tags to identify and describe the image.

DICOM has an information model which differentiates it from other standards used in the medical industries sector. The model is based on 'information objects' which include definitions (an information template) on the information to be exchanged. Each image type, and therefore information object, has specific characteristics. A CT image, for example, requires different descriptors in the image header compared to an ultrasound image or an ophthalmology image. These templates are identified by unique identifiers, which are registered by the National Electrical Manufacturers Association, the DICOM standard facilitator. Information objects are also known as part of the Service Object Pairs (SOP) Classes. An example of a SOP Class is the CT Storage SOP Class, which allows CT images to be exchanged.

DICOM includes a robust protocol where each DICOM command is acknowledged thereby providing an implicit version control. Strict guidelines are employed requiring each DICOM compatible device to describe its functionality, including supported SOP Classes and transfer syntaxes in a document called the DICOM Conformance Statement. This document allows a user to determine in advance whether or not a specific device is compatible with other devices. Conformance statements contain details about exception and error handling and often contain complete specifications for the information objects (e.g. images) that are exchanged. DICOM uses information management services which include a Modality Work List allowing scheduling information to be retrieved by a modality. The other service in this category is the DICOM Storage Commitment, which transfers the responsibility for images to the receiver, so they can be safely removed from the local disk.

Image quality is the principal issue with regard to the DICOM standardization. DICOM achieves consistency in the image presentation on different monitors, as well as on film, independent of the make or type of characteristics of the medium using the DICOM Greyscale Standard Display Function. This function specifies exactly what luminance or density level should be produced for a certain input value, based on the *Barten curve*, which maps the values into a range that is perceptually linear. This means that input values are mapped into a space that is perceived as linear by a human observer.

In addition to the principal objectives of the DICOM standard for image visualization, it includes structured reporting which is an object that can be exchanged, very similar to an image, except that instead of pixel data, the message body is a Structured Report. Finally DICOM facilitates security mechanism including access control and authorization rules implemented by the application level software using passwords or biometric access controls coupled with an audit and logging mechanism.

There are a number of DICOM viewers available which allow medical images to be displayed, processed and analyzed. Among the most advanced and versatile of these 'viewers' is the OsiriX imaging software which is limited only in its requirement for implementation in a Unix/Linux environment, thereby making use of the advanced graphics facilities that accompany an Apple Mac, for example.

III. The OsiriX DICOM Viewer

OsiriX is an advanced open-source DICOM viewer for visualizing and processing images produced by a range of medical imaging systems [7] including MR and CT, Position Emission Tomography (PET), PET-CT, ultrasonic B-Scan imaging and so on [8]. Designed for uses under a Unix/Linux operating system, it is arguably the world's most widely used and versatile medical imaging processing and visualization system and is fully compliant with the DICOM standard for image communication and image file formats.

OsiriX has been specifically designed for navigation and visualization of multimodality and multidimensional images. It incorporates basic 2D viewing, a 3D viewer and 4D viewer (a 3D series with temporal dimension such as Cardiac-CT, for example) and a 5D viewer (3D series with temporal and functional dimensions; for example, Cardiac-PET-CT). The 3D viewer offers all modern rendering modes including Multi-Planar Reconstruction (MPR), Surface Rendering, Volume Rendering and Maximum Intensity Projection (MIP). All these modes support 4D data and are able to produce Image Fusions between different series of images.

The current version of OsiriX provides all aspects of DICOM file support and has a built-in SQL (Structured Query Language) compatible database with an unlimited number of files. Fully compatible network support is provided and the system is available as a 32-bit or 64-bit version. It has an intuitive GUI (Graphical User Interface) with customizable Toolbars and includes multi-slice CT and MR imaging with Regions of Interest (ROI) including Polygons, Circles, Pencil, Rectangles and Points with undo/redo. The 3D Post-Processing facilities of OsiriX include MIP (Maximum Intensity Projection), Volume Rendering, Surface Rendering, ROI, Texture Mapping, Image Registration and Stereo Vision (using glasses).

OsiriX provides custom CLUT (Color Look-Up Tables), 3×3 and 5×5 FIR (convolution) filters (e.g. a 'Bone filter'), a 4D viewer for Cardiac-CT and other temporal series and Image Fusion for PET-CT examinations, for example, with adjustable blending percentage. With regard to the work reported in this paper, OsiriX provides a complete dynamic Plugin architecture for external functions used for expansion and scientific research. This includes the creation and management of OpenGL views.

[1] An edited version of the DICOM standard, overview and characteristics: a whitepaper.

Figure 1 shows an example of the OsiriX DICOM Viewer illustrating the visualization of a PET image for the whole body and a CT scan of the head and upper torso. The use of combining data from CT scans (which provide high resolution images of both bone and soft tissues) and PET scans (which allows images to be derived on areas of the body that have been doped with radioactive isotopes of Oxygen, Carbon and Nitrogen, for example, with short half-lives) requires pixel and voxel registration using Image Fusion methods for which OsiriX provides an ideal programming environment [9]. OsiriX also has powerful volume rendering, surface and ROI visualization facilities. For example, Figure 2 shows a 3D rendered image from a CT scan of the middle torso.

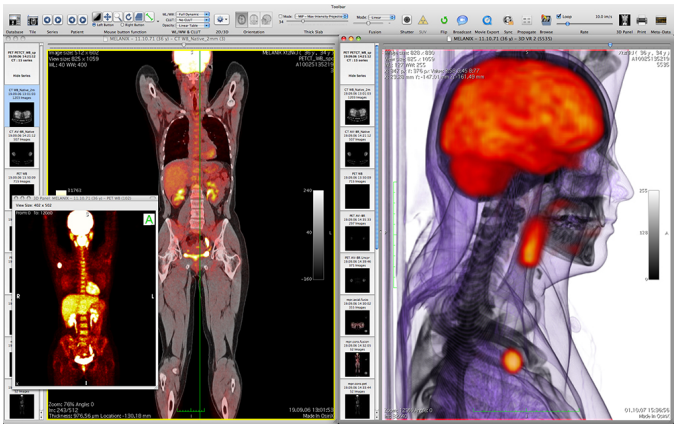

Fig. 1. Screen shot of PET-CT images using the OsiriX DICOM Viewer.

Fig. 2. Screen shot of a 4D volume rendered CT image using the OsiriX DICOM Viewer.

A version of OsiriX is also available for the iPhone although is functionality is currently limited to low data volume visualization [10].

IV. Noise Sources in CT, PET and MR Imaging

CT, PET and MR images contain characteristic noise fields that are derived from a combination of effects due to a range of disturbances and interference that effect the signal detection and/or are an inherent component of the signals recorded. Because noise is multifaceted, it is not possible to define it uniquely. For this reason, statistical models are required to construct a suitable Probability Density Function for the noise which is statistically compatible with the data. However, as a consequence of the Central Limit Theorem, where the addition of many independent noise fields yields a resultant field that is Gaussian distributed, the noise fields in CT, MR and PET images is often taken to be Gaussian. However, there is a particular component of the noise in these imaging modalities that is unique in that it is a consequence of the image reconstruction method that is required. This is concerned with the underlying model used to describe a set of projections $P(\hat{\mathbf{n}}, z)$ in the plane (where $\hat{\mathbf{n}}$ is the unit vector pointing along the path of a projection) which is given by the Radon transform [11]

$$P(\hat{\mathbf{n}}, z) = \int_{-\infty}^{\infty} f(\mathbf{r})\delta(z - \hat{\mathbf{n}} \cdot \mathbf{r}) d^2\mathbf{r}$$

where $f(\mathbf{r})$ is some 2D object function which is related to the physical basis of the imaging modality (e.g. X-ray absorption in the case of X-ray CT). This transform describes a set of parallel projections (line integrals) taken over all angles between 0 and 180^o. The inverse Radon transform is given by [11], [12]

$$f(\mathbf{r}) = \frac{1}{2\pi^2} \int_0^{\pi} d\theta \int_{-\infty}^{\infty} dz \frac{1}{\hat{\mathbf{n}} \cdot \mathbf{r} - z} \frac{\partial}{\partial z} P(\hat{\mathbf{n}}, z)$$

This transform is the theoretical basis for parallel beam CT and PET although it should be noted that latter 'fourth generation' CT and most current systems are based on fan beam project tomography [13]. With regard to MR imaging, image reconstruction is typically undertaken using so called k-space (spatial frequency space) methods which are related to the Central Slice Theorem for the Radon transform [11].

Irrespective of the method used to reconstruct a CT, PET or MR image, numerical errors occur that are essentially a consequence of the need to map data in a polar or partially polar coordinate system into a Cartesian system. This is because of the intrinsic geometry of the imaging systems that are used where the recorded data has some angular dependence relative to the object function - the body. Although various filters are available to reduce the numerical errors that occur subject to a given resolution (which depends on the angular step change), for example, the fact that some form of numerical error is inevitable yields a characteristic noise field, particularly in the case of CT and PET. In the case of MR imaging, the noise fields are the result of more complex processes which include the effect of diffusion associated with the time taken to record the data and the intensity (amplitude) of the recorded signals which depend on the strength of the magnetic field and the RF fields used to induce proton gyration [14]. Figure 3 provides examples of noise fields that are characteristic of parallel beam and fan-beam (fourth generation) CT. In these examples, the projections are generated from a uniform image (with all pixels

values set to 1) and the reconstructions (computed using a complete set of projections from 0-179 degrees inclusively in steps of 1 degree) have been histogram equalized for the purpose of vizualising the noise patterns produced.

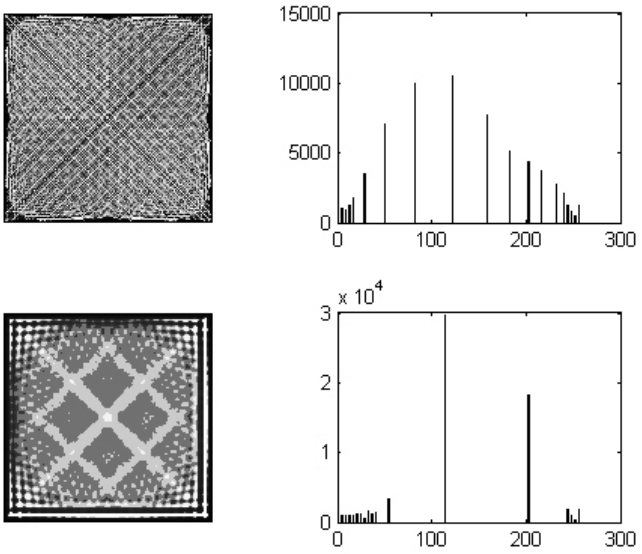

Fig. 3. Example of the characteristic noise fields produced by a parallel beam reconstruction (top-left) using nearest neighbour Polar-to-Cartesian coordinate interpolation and the corresponding 256-bin histogram (top-right) after application of histogram equalization. The equivalent fan beam reconstruction and the corresponding histogram are given in the bottom-left and bottom-right quadrants of the figure, respectively.

V. Evolution of Random Processes, Diffusion and Noise

Anisotropic Diffusion describes diffusion processes where the Diffusivity is not a constant but may very in space (Isotropic Inhomogeneous Diffusion when the Diffusivity is a scalar function of space) and whose spatial variations may be directional (Non-isotropic Inhomogeneous Diffusion when the Diffusivity is a Vector or Tensor function of space). In both cases the governing equation is the Diffusion equation and in this section we briefly look at the origins of this equation. In particular, we investigate the origins of the classical diffusion equation and the fractional diffusion equation. The purpose of this is to inform the reader of the different physical processes that are assumed in the derivation of the classical and fractional diffusion equations in which the fractional diffusion equation can be taken to be a generalization.

A. Einstein's Evolution Equation

In [15], the following evolution equation is considered

$$u(\mathbf{r}, t+\tau) = u(\mathbf{r}, t) \otimes_{\mathbf{r}} p(r), \quad r \equiv \mid \mathbf{r} \mid = \sqrt{x^2 + y^2 + z^2} \quad (1)$$

where $\otimes_{\mathbf{r}}$ denotes the convolution integral over all space (denoted by the vector $\mathbf{r}$), $u(\mathbf{r}, t)$ the 'Density Field' which describes the distribution of a canonical ensemble of particles undergoing elastic scattering and p denotes the Probability Density Function (PDF). The space-time evolution of the Density Field $u(\mathbf{r}, t)$ depends upon the PDF that characterizes the statistical behaviour associated with the elastic scattering processes in terms of each particle in the canonical ensemble of particles undergoing a three-dimensional random walk.

Einstein's evolution equation is, in a conventional sense, related to the concept of particle interactions responsible for generating Brownian motion, for example. However, the same evolution equation can be considered in the context of light rays, for example, interacting with a population of random point scatterers where the density field is taken to be a measure of the intensity of the scattered light. In imaging theory, multiple scattering is taken to contribute to the noise term of the fundamental imaging equation where the recorded image is given by the convolution of the Object Function with the Point Spread Function of the imaging system plus noise. The convolution term models single scattering processes according to the Born or Kirchhoff approximations (for volume and surface scattering problems, respectively). However, in general, any imaging system is usually taken to conform to this model and the noise term may be generalized in terms of some product of an effect that is interpreted on a statistical basis. This includes the statistical model compounded in Einstein's evolution equation, which, in this paper, forms the basis associated with the algorithms developed for reducing the effects of diffusion in CT and MR images.

B. Derivation of the Classical and Fractional Diffusion Equations

The classical diffusion equation can be derived from equation (1) by using a Taylor expansion of the density field $u(\mathbf{r}, t+\tau)$ and the convolution integral. This is the basis for Einstein's derivation of the diffusion equation from which the Diffusivity and Diffusion Tensors are constructed. Here, we consider a different approach which serves to provide a unifying theme for understanding the concept of Gaussian and non-Gaussian diffusion.

Using the convolution theorem, equation (1) can be written in Fourier space as

$$\widetilde{u}(\mathbf{k}, t+\tau) = \widetilde{u}(\mathbf{k}, t)\widetilde{p}(k), \quad k \equiv \mid \mathbf{k} \mid = \sqrt{k_x^2 + k_y^2 + k_z^2} \quad (2)$$

where $\widetilde{u}$ and $\widetilde{p}$ denote the Fourier transforms of u and p, respectively ($\widetilde{p}$ being referred to as the Characteristic Function, a conventional term in statistics and statistical mechanics), and k_x, k_y and k_z are the spatial frequencies in a Cartesian coordinate system.

Clearly, the properties of the Characteristic Function $\widetilde{p}$ determine the statistical characteristics of the 'system', which, in turn, defines the evolution of the density field $u(\mathbf{r}, t)$ via equation (1). For a homogeneous Gaussian system and for some real constant $a > 0$, $\widetilde{p}(k) = \exp(-ak^2)$. We can generalize this result and consider the Lévy Characteristic Function $\widetilde{p}(k) = \exp(-ak^\gamma)$ where $\gamma \in (0, 2]$ is the Lévy index. However, this generalization does not take into account the fact that the diffusing properties of the 'system' can be inhomogeneous. We therefore generalize further and consider the Characteristics Function

$$\widetilde{p}(\mathbf{k}) = \exp[-\widetilde{a}(\mathbf{k}) \otimes_{\mathbf{k}} k^\gamma] \quad (3)$$

where $\otimes_{\mathbf{k}}$ denotes the convolution integral over all $\mathbf{k}$-space which reduces to the homogeneous case when $\widetilde{a}(\mathbf{k}) = a\delta^3(\mathbf{k})$ where δ^3 denotes the 3D Dirac delta function.

Given equations (2) and (3), we can now derive the inhomogeneous fractional diffusion equation which is based on:

(i) Taylor expanding $\widetilde{u}(\mathbf{k}, t+\tau)$ to first order so that

$$\widetilde{u}(\mathbf{k}, t+\tau) \simeq \widetilde{u}(\mathbf{k}, t) + \tau \frac{\partial}{\partial t}\widetilde{u}(\mathbf{k}, t)$$

(ii) Considering a first order approximation to the exponential function of the form

$$\widetilde{p}(\mathbf{k}) \simeq 1 - \widetilde{a}(\mathbf{k}) \otimes_{\mathbf{k}} k^{\gamma}$$

(iii) Using the Reisz definition of a fractional Laplacian, i.e.

$$\nabla^{\gamma} \leftrightarrow -k^{\gamma}$$

where $\leftrightarrow$ denotes transformation from real-space to $\mathbf{k}$-space.

Using these results we derive the equation

$$\frac{\partial}{\partial t}u(\mathbf{r}, t) = D(\mathbf{r})\nabla^{\gamma}u(\mathbf{r}, t) \tag{4}$$

where $D(\mathbf{r}) = a(\mathbf{r})/\tau$ is the (fractional) 'Diffusivity' and we have used the result

$$[\widetilde{a}(\mathbf{k}) \otimes_{\mathbf{k}} k^{\gamma}]\widetilde{u}(\mathbf{k}, t) \leftrightarrow [a(\mathbf{r})\delta^{\gamma}(\mathbf{r})] \otimes_{\mathbf{r}} u(\mathbf{r}, t)$$

and noted that, by Taylor expanding the function a (within the convolution integral), then, for a unit vector $\hat{\mathbf{n}}$,

$$[a(\mathbf{r})\delta^{\gamma}(\mathbf{r})] \otimes_{\mathbf{r}} u(\mathbf{r}, t) = a(\mathbf{r})[\delta^{\gamma}(\mathbf{r}) \otimes_{\mathbf{r}} u(\mathbf{r}, t)]$$

$$+\nabla a(\mathbf{r}) \cdot \hat{\mathbf{n}}\nabla^{\gamma}[ru(\mathbf{r}, t)] + ... \sim -a(\mathbf{r})\nabla^{\gamma}u(\mathbf{r}, t), \quad r \to 0$$

For a Gaussian distributed 'system' equation (4) reduces to the classical inhomogeneous diffusion equation when $\gamma = 2$. For $\gamma < 2$, equation (4) models a 'system' where the density function is the 'product' of a canonical ensemble of trajectories (particles of light-rays) that have a propensity for propagating over longer distances in an interval of time τ. This effect is compounded in the long tail distributions associated with the case when $\gamma < 2$ in equation (3) subject to the inhomogeneous nature of the system compounded in the function $\widetilde{a}(\mathbf{k})$ which determines the Diffusivity D (apart from scaling by $1/\tau$).

VI. Noise Reduction using Anisotropic Diffusion

We consider the application of equation (4) in two-dimensions for the suppression of noise in an image $u(x, y)$ which has been sampled to form a digital image consisting of a uniformly sampled array of pixels u_{ij}.

A. Solution for $\gamma = 2$

For $\gamma = 2$, equation (4) is

$$\frac{\partial}{\partial t}u(x, y, t) = D(x, y)\nabla^2 u(x, y, t)$$

A numerical solution is considered that is based on solving the above equation using a time step $\delta \equiv \delta t$. Forward differencing in time and centre differencing in space (for a uniformly sampled grid with sampling intervals of Δx and Δy) we obtain

$$\frac{u_{ij}^{k+1} - u_{ij}^{k}}{\delta} = \frac{D_{ij}}{\Delta^2}(u_{i+1,j} + u_{i-1,j} + u_{i,j+1} + u_{i,j-1} - 4u_{ij})$$

where $\Delta \equiv \Delta x = \Delta y$. Rearranging this result, we obtain the iterative solution

$$u_{ij}^{k+1} = u_{ij}^{k} + \lambda D_{ij} \times L_{ij} \otimes_{i,j} u_{ij}^{k}, \quad k = 0, 1, 2, ..., N \tag{5}$$

where $\lambda = \delta/\Delta^2$ is the 'time space-squared step ratio', N is the total number of iterations and

$$L_{ij} = \begin{pmatrix} 0 & 1 & 0 \\ 1 & -4 & 1 \\ 0 & 1 & 0 \end{pmatrix} \tag{6}$$

The matrix L_{ij} defines the Laplacian Finite Impulse Response (FIR) filter of this iterative system where $\otimes_{i,j}$ denotes the discrete convolution sum over all i and j. The initial value u_{ij}^{0} is taken to be the original (noisy) image.

B. Solution for $\gamma \in (0, 2)$

A solution to this problem has previously been considered by [16] using a Fourier transform based approach and implemented using a FFT (Fast Fourier Transform) based algorithm. In this paper, we consider an approximation required to implement the method of solution using a FIR filter. The 'key' to this approach is to note that $\nabla^{\gamma} \equiv \nabla^2\nabla^{\gamma-2}$ so that the FIR filter given by equation (6) can be used and applied to the computation of $\nabla^{\gamma-2}u(x, y, t)$. The computation of this term is based on the following two-dimensional Fourier transform relationship [17]

$$\frac{1}{r^{\gamma}} \leftrightarrow \frac{\Gamma_{\gamma}}{k^{2-\gamma}} \tag{7}$$

where

$$\Gamma_{\gamma} = \frac{2^{2-\gamma}\pi\Gamma\left(1 - \frac{\gamma}{2}\right)}{\Gamma\left(\frac{\gamma}{2}\right)}, \quad r = \sqrt{x^2 + y^2}, \quad k = \sqrt{k_x^2 + k_y^2}$$

Using the Reisz definition for a fractional Laplacian,

$$\nabla^{\gamma-2}u(\mathbf{r}, t) \leftrightarrow k^{\gamma-2}\widetilde{u}(\mathbf{k}, t) = \frac{\widetilde{u}(\mathbf{k}, t)}{k^{2-\gamma}}, \quad 0 < \gamma < 2$$

from which, given relationship (7) and using the convolution theorem, it follows that

$$\nabla^{\gamma-2}u(x, y, t) = \frac{1}{\Gamma_{\gamma}(x^2 + y^2)^{\gamma/2}} \otimes_{x,y} u(x, y, t)$$

We can now approximate the convolution kernel to form a FIR filter (of an odd order) where, for a rectangular grid, the singularity is taken to occur at $(1, 1)$. Under these conditions, and, with $\alpha = \gamma/2$, we can consider an order 3 FIR filter of the form

$$M_{ij}^{3}(\alpha) = \frac{1}{\Gamma_{2\alpha}} \begin{pmatrix} 8^{-\alpha} & 5^{-\alpha} & 8^{-\alpha} \\ 5^{-\alpha} & 2^{-\alpha} & 5^{-\alpha} \\ 8^{-\alpha} & 5^{-\alpha} & 8^{-\alpha} \end{pmatrix}$$

and an order 5 FIR filter of the form

$$M_{ij}^5(\alpha) = \frac{1}{\Gamma_{2\alpha}} \begin{pmatrix} 18^{-\alpha} & 13^{-\alpha} & 10^{-\alpha} & 13^{-\alpha} & 18^{-\alpha} \\ 13^{-\alpha} & 8^{-\alpha} & 5^{-\alpha} & 8^{-\alpha} & 13^{-\alpha} \\ 10^{-\alpha} & 5^{-\alpha} & 2^{-\alpha} & 5^{-\alpha} & 10^{-\alpha} \\ 13^{-\alpha} & 8^{-\alpha} & 5^{-\alpha} & 8^{-\alpha} & 13^{-\alpha} \\ 18^{-\alpha} & 13^{-\alpha} & 10^{-\alpha} & 13^{-\alpha} & 18^{-\alpha} \end{pmatrix}$$

where higher order filters are constructed similarly. In each case, the forward differenced in time solution to equation (4) is given by (where n is the order of the filter)

$$u_{ij}^{k+1} = u_{ij}^k + \lambda D_{ij} \times L_{ij} \otimes_{i,j} M_{ij}^n(\alpha) \otimes_{i,j} u_{ij}^k \qquad (8)$$

where u_{ij}^0 is taken to be the input image.

C. Computation of the Diffusivity

In the context of processing a digital image u_{ij}^0, application of equations (5) and (8) depend critically upon the generation of the array D_{ij}. In the absence of any *a priori* information (which is the usual case) this array must be obtained from the image u_{ij}^0. With regard to using equations (5) and (8) for noise reduction, the value of D_{ij} at any pixel location (i, j) can be used to control the degree of diffusion, which, in terms of a diffusion process, represents the degree of blurring in the locality of (i, j). For correlated features in an image that are edge dominant and are taken to be relatively noise free (at least, in terms of their high pixel value contrast with regard to low pixel value background noise), we require the degree of diffusion to decrease. This can be accomplished by reducing the value of D_{ij} in regions of an image that are edge dominant and increasing the value of D_{ij} in those regions that are background noise dominant. A method of achieving this is to apply an edge detector to the image u_{ij}^0 to obtain an output E_{ij}, say, and compute

$$D_{ij} = 1 - E_{ij} \qquad (9)$$

where E_{ij} is (intensity) normalized, i.e. $0 \leq E_{ij} \leq 1 \quad \forall(i, j)$ so that $D_{ij} \in [0, 1] \quad \forall(i, j)$.

There are a range of edge detection filters that can be applied in this respect to compute D_{ij} [17]. Further, binarization of equation (9) can be applied via application of a standard thresholding method, i.e. for a *Threshold* $0 < T < 1$,

$$D_{ij} = \begin{cases} 1, & 1 - E_{ij} > T \\ 0, & 1 - E_{ij} \leq T \end{cases} \qquad (10)$$

The issue of which edge detection filter to use and whether or not to binarize the output based on the application of equation (10) or to apply a variable threshold approach lies beyond the scope of this paper. As with other image processing applications, the filter(s) depends on a detailed appraisal of the data. This includes image acquisition, the application focus and user preferences. Edge detection methods are designed to provide a balance between the fidelity of the output in terms of edge accuracy, localization and continuity and the effects of noise leading to spurious edges. In this application, edge detection is being applied for the purpose of non-stationary noise reduction rather than pattern recognition. Further, because the current application is focused on clinical image analysis in real time, it is not appropriate to provide the user with a range of filters for edge detection including parameter settings etc. Rather, we require a hardwired solution that is efficient with minimal computational cost. In this context, second order edge detection via the Marr-Hildreth algorithm [18], for example, or first order edge detection requiring pre-filtering, such as the Canny edge detector [17] is not suitable (at least in a first study as provided in this paper. We therefore consider a well known and simple but effective edge detector, namely, on the Sobel filter which is based on the application of the FIR gradient filters

$$G_x = \frac{1}{8} \begin{pmatrix} -1 & 0 & 1 \\ -2 & 0 & 2 \\ -1 & 0 & 1 \end{pmatrix}, \quad G_y = \frac{1}{8} \begin{pmatrix} -1 & -2 & -1 \\ 0 & 0 & 0 \\ 1 & 2 & 1 \end{pmatrix}$$

For an input image u_{ij}^0, the output is given by

$$G_{ij} = \mid G_x \otimes_{i,j} u_{ij}^0 \mid + \mid G_y \otimes_{i,j} u_{ij}^0 \mid$$

which is then normalized to yield E_{ij} as follows:

$$E_{ij} = \frac{G_{ij}}{\max(G_{ij})}$$

from which the Diffusivity can be obtained via equations (9) and (10) using a 50% threshold, i.e. $T = 0.5$.

Number of Iterations N	Time-Space Step Ratio λ	Lévy Index γ	Threshold T
20	0.01	1.5	0.5

TABLE I

VALUES OF 'HARD-WIRED' PARAMETERS FOR THE OSIRIX ANISOTROPIC DIFFUSION PROCESSING FILTER.

VII. IMPLEMENTATION IN OSIRIX IMAGE PROCESSING SOFTWARE

OsiriX provides the facility for programming filters using the XCode Apple Developer C/C++ compiler [19]. Implementation of the algorithms discussed in the previous sections, in particular equation (8), is easily converted to C-code for implementation in an OsiriX programming environment. The current processor, the OsiriX Anisotropic Diffusion Processor (OADP), is available on-line at [20].

The OADP filter has been designed to be easy to implement and integrate in OsiriX as a Plugin and to be use by a radiologist. No parameter settings are required which comes at the expense of the user being unable to optimize the filter and investigate its properties in a dynamic and image dependent sense. However, these options are not suitable for the medical imaging practitioner who typically expects the operational criteria of a filter to be hard-wired. The current parameters are hard-wired according to Table I. Figure 4 shows an example screen shot after application of the OsiriX OADP filter for a typical CT image using the Plugin application file available at [20]. Figure 5 shows an example of using the OsiriX 3D volume rendering facility after applying a crop to locate a Brain tumour using MR image data to which the OADP filter has been applied. As a final example, Figure 6 shows the result of applying the OsiriX surface rendering option. The

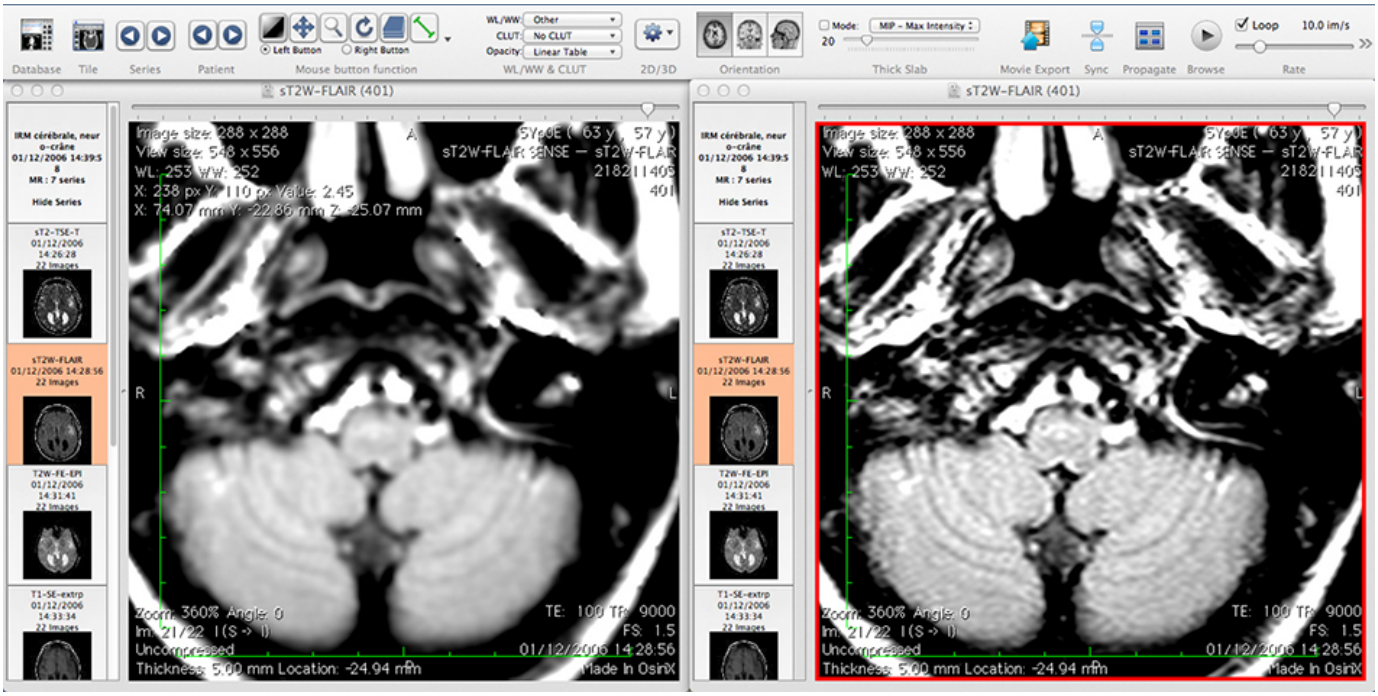

Fig. 4. Screen shot of the OsiriX imaging processing software after application of the Anisotropic Diffusion Processor (left) applied to a standard CT image (right) of the Cerebellum (base of the Brain).

image consists of two Iso-surfaces with equal transparency weighting, generated using CT data processed with the OADP filter.

VIII. Conclusions

We have investigated the principles associated with the Anisotropic Diffusion Method for noise reduction and extended the approach to include the case when the underlying statistical models for random walk processes are non-Gaussian. For the case when these processes are taken to be described by a Lévy distribution, a new n^{th}-order FIR filter M_{ij}^{n} (where $n = 3, 5, ...$)has been derived in Section 6.2. The approach to deriving these filters (as presented in Section 5.2) is general and can therefore, in principle, be used to design filters for different Characteristic Functions. However, it should be noted that the Lévy function considered in this paper is approximated in order to undertake the analysis that is applied and that higher order results should be further investigated with regard to the design and implementation of different filters.

Irrespective of whether the Anisotropic Diffusion Method is based on a Gaussian or non-Gaussian model, the algorithms compounded in equations (5) and (8), respectively, are predicated on being able to obtain an estimate of the Diffusivity. This is typically undertaken through application of an edge detection method, and, in this paper, we have consider the Sobel edge detection algorithm. However, there is considerable scope for investigating further edge detection methods for this purpose (which lie beyond the scope of this paper). In particular, given the binarization condition that has been applied via equation (10), application of the Marr-Hildreth second order edge detection algorithm may be of value in this context given that edge continuity tends to be preserved in this case. However, it should be noted that the application of second order edge detection for computing the Diffusivity comes at the expense of greater computational overheads and an increase in parameter optimization, in particular, the bandwidth that is applied.

The principal focus of the algorithm developed in this paper has been its implementation in a real time medical image processing environment. For this purpose, the OsiriX DICOM Viewer has been chosen because of the existing and extensive facilities that this system provides, its universal appeal and the programming environment that is available. In this context, the paper has reported on the development of a new OsiriX DICOM filter for noise reduction using a non-Gaussian anisotropic diffusion model. Readers can investigate this approach further by implementing the application available via [20] within the Osirix operational environment [8]. This application includes operational conditions that transcend the results presented in this paper and provides the user with additional options for investigating the performance of the filters considered in this paper.

Acknowledgments

The research reported in this paper is supported by the Science Foundation Ireland Stokes Professorship Programme. The authors also acknowledge the support of Institute of Cancer Research and Dublin Institute of Technology.

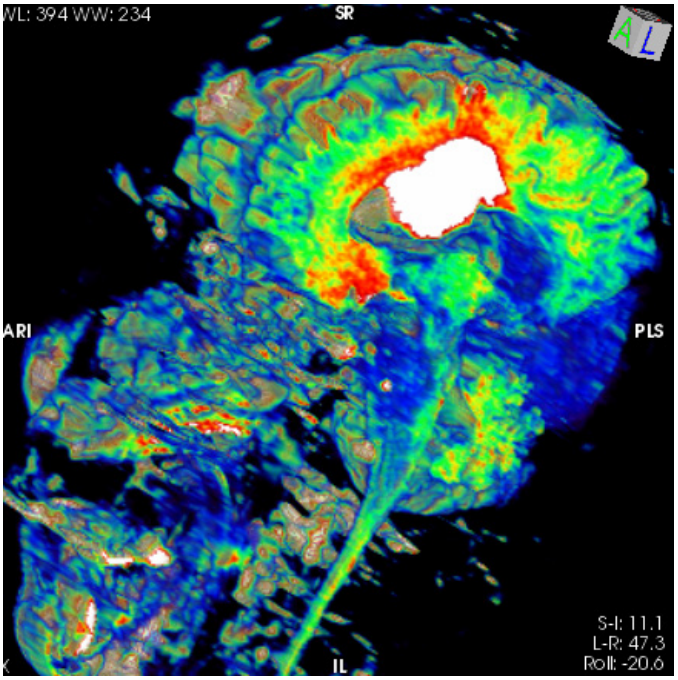

Fig. 5. Example of the OsiriX Anisotropic Diffusion Processor applied to MR image data using the OsiriX 3D Volume Rendering and cropping facility to highlight a brain tumour (white region in the top-half of the image) with CLUT: Spectrum.

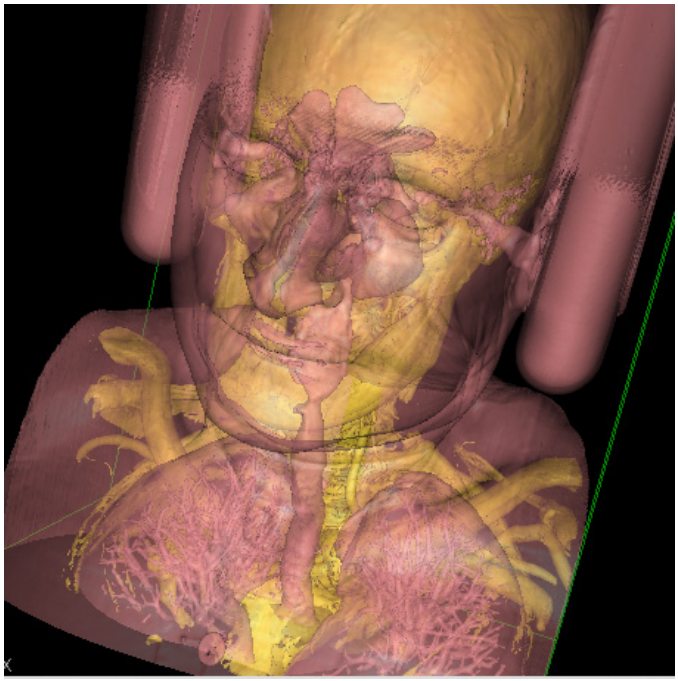

Fig. 6. Example of the OsiriX Anisotropic Diffusion Processor applied to CT data using the OsiriX Surface Rendering facility to generate an Iso- surface consisting of two surfaces with equal transparencies.

REFERENCES

[1] D. A. Ortendahl, N. M. Hylton, L. Kaufman, and L. E. Crooks, "Signal to noise in derived magnetic resonance images," *Magnetic Resonance in Medicine*, vol. 1, pp. 316–338, 1984.

[2] D. M. Koh and D. J. Collins, "Diffusion-weighted mri in the body: Applications and challenges in oncology," *American Journal of Roentgenology*, vol. 188, pp. 1622–1635, 2007.

[3] T. G. Reese, O. Heid, R. M. Weisskoff, and V. J. Wedeen, "Reduction of eddy-current-induced distortion in diffusion mri using a twice-refocused spin echo," *Magnetic Resonance in Medicine*, vol. 49, pp. 177–82, 2003.

[4] T. Takahara, D. M. Koh, Y. Imai, and D. J. Collins, "Practical aspects of assessing tumours using clinical diffusion weighted imaging in the body," *Magnetic Resonance Medical Science*, vol. 6, pp. 211–24, 2007.

[5] P. Kingsley, "Introduction to diffusion tensor imaging mathematics, part iii: Tensor calculation, noise, simulations and optimization," *Concepts in Magnetic Resonance A*, vol. 28A, pp. 155–179, 2006.

[6] "Digital imaging and communications in medicine." `http://medical.nema.org`, 2012.

[7] J. M. Blackledge, "Medical imaging: Image acqisition, processing and clinical applications." `http://eleceng.dit.ie/jblackledge/MedicalImaging.zip`, 2011.

[8] A. Amanullah, P. Justen, A. Davies, G. C. Paul, A. W. Nienow, and C. R. Thomas, "Osirix imaging software: Advanced open-source pacs workstation dicom viewer." `http://www.osirix-viewer.com`, 2012.

[9] PET-CT, "Positron emission tomography and ct image fusion." `http://www.osirix-viewer.com/PICTS/Fusion.mov`, 2012.

[10] iPhone OsiriX, "Osirix for iphone." `http://www.osirix-viewer.com/MobileOsiriXPreview.mov`, 2012.

[11] S. R. Deans, *The Radon Transform and Some of Its Applications*. Wiley, 1983.

[12] F. Natterer, *The Mathematics of Computerized Tomography*. Wiley, 1986.

[13] G. T. Herman, *Image Reconstruction for Projections*. Academic Press, 1980.

[14] M. D. Blackledge, *Assessing Response in Bone Metastases using Diffusion Weighted MRI*. PhD Thesis, University of London, 2012.

[15] A. Einstein, "On the motion of small particles suspended in liquids at rest required by the molecular-kinetic theory of heat," *Annalen der Physik*, vol. 17, pp. 549–560, 1905.

[16] J. M. Blackledge and M. D. Blackledge, "Fractional anisotropic diffusion for noise reduction in magnetic resonance images," *Transactions on Electronics and Signal Processing*, vol. 4, no. 1, pp. 44–57, 2012.

[17] J. M. Blackledge, *Digital Image Processing*. Horwood Publishing, 2005.

[18] D. Marr, "On the theory of edge detection," *Proceedings of the Royal Society*, vol. B, no. 207, pp. 127–217, 1980.

[19] AppleMac, "Xcode for the apple mac." `http://www.macupdate.com/app/mac/13621/apple-xcode`, 2012.

[20] J. M. Blackledge, M. D. Blackledge, and J. N. Coutney, "Osirix anisotropic diffusion processor." `http://eleceng.dit.ie/jblackledge/OADP.zip`, 2012.

Jonathan Blackledge graduated in physics from Imperial College in 1980. He gained a PhD in theoretical physics from London University in 1984 and was then appointed a Research Fellow of Physics at Kings College, London, from 1984 to 1988, specializing in inverse problems in electromagnetism. During this period, he worked on a number of industrial research contracts undertaking theoretical and computational research into the applications of inverse scattering theory for the analysis of signals and images. In 1988, he joined the Applied Mathematics and Computing Group at Cranfield University as Lecturer and later, as Senior Lecturer and Head of Group where he promoted postgraduate teaching and research in applied and engineering mathematics in areas which included computer aided engineering, digital signal processing and computer graphics. In 1994, Jonathan Blackledge was appointed Professor of Applied Mathematics and Head of the Department of Mathematical Sciences at De Montfort University where he expanded the post-graduate and research portfolio of the Department and established the Institute of Simulation Sciences. From 2002-2008 he was appointed Visiting Professor of Information and Communications Technology in the Advanced Signal Processing Research Group, Department of Electronics and Electrical Engineering at Loughborough University, England (a group which he co-founded in 2003 as part of his appointment). In 2004 he was appointed Professor Extraordinaire of Computer Science in the Department of Computer Science at the University of the Western Cape, South Africa. He currently holds the prestigious Stokes Professorship under the Science Foundation Ireland Programme based in the School of Electrical Engineering Systems, Dublin Institute of Technology and is Distinguished Professor at the Centre for Advanced Studies, Warsaw University of Technology, Poland.

Matthew Blackledge graduated with a degree in Physics from Imperial College, London in 2006. He moved on to pursue a career in medical imaging and completed a Masters Degree in Medical Physics with distinction from the University of Surrey in 2007. After undertaking research into Diffusion Weighted Magnetic Resonance Imaging (MRI) working with the Cancer Imaging Centre at the Institute of Cancer Research (ICR) and Royal Marsden Hospital, he was awarded a PhD from the University of London in 2012 for a thesis entitled *Assessing Response in Bone Metastases using Diffusion Weighted MRI*. He is now a Research Fellow at the ICR with research interests that include the acquisition and post-processing of Diffusion Weighted MRI focusing on their application for the detection of brain tumours, full-body medical imaging and combined MRI/CT/PET imaging. Teaching duties include the provision of short course programmes in Medical Physics, Software Engineering and Imaging Processing for Clinical Diagnosis.

Jane Courtney graduated with a degree in Electrical Engineering from University College Dublin (UCD) in 1998. After a year working as a project engineer in industry, she returned to UCD to pursue research in biomedical engineering and graduated with a Masters Degree in 2001 and a Doctorate in 2005. Her research has focused on using digital image processing to develop a novel gait analysis system. Current research and teaching interests include computer vision and image processing, biomedical engineering and power systems engineering. In 2004, she taught on the intervarsity MSc in biomedical engineering. She has been a member of several programme committees including the Medical Imaging and Telemedicine Conference held in FuJian, China, in August 2005, the International Machine Vision and Image Processing conference in 2006, 2007 and 2011 and the Ninth International Conference on Environment and Electrical Engineering held in Prague in May 2010. She was also a reviewer for the European Conference on Circuit Theory and Design held in August 2005 and is currently a reviewer for the Journal of Biomechanics. She is part of the Health Engineering and Rehabilitation Team and People Oriented Technology Research groups at Dublin Institute of Technology (DIT) and an adjunct member of the Vision Systems Group, Dublin City University. From September 1999 to April 2001, Jane worked as an assistant lecturer in the Department of Electrical Engineering in DIT. While pursuing her PhD, she worked as a lecturer in the Department of Electronic and Electrical Engineering at UCD returning to DIT as a full-time lecturer in September 2004.